JOURNAL OF MATERIALS SCIENCE 7 (1972) 1391–1400

The critical current density of deformed and annealed superconducting Nb-26% Zr and Nb-32% Zr and its dependence on the amount of deformation

T. R. FINLAYSON*, I. MILNE
Central Electricity Research Laboratories, Kelvin Avenue, Leatherhead, Surrey, UK

A study of the low-field critical current densities (computed from magnetization data) which can be achieved by heat-treating for 1 h Nb-Zr alloys deformed various amounts, has shown that a peak critical current density is always reached after annealing at around 750°C. The magnitude of this peak depends upon the amount of deformation, but is not increased by deforming beyond 80%. Superconducting transition temperatures are also reported.

The microstructure was unusual in that deformation was very unevenly distributed and there was little tendency for the dislocations to cross-slip or to form a cellular structure. Precipitation of β_{Zr} occurred in regions of high deformation only, so that equilibrium was not achieved below 80% deformation. The measured superconducting properties are explained in terms of this microstructure, with β_{Zr} as the dominant flux pinning agent.

1. Introduction

Interest in hard type II superconductors has recently been stimulated by the need to produce a material to carry overload currents in a superconducting A.C. power transmission cable [1]. The zero-field critical current density is one of the most convenient parameters which can be used to classify materials for the above purpose, and it has been shown that in Nb-Zr alloys this is controlled mainly by the dispersion of the flux pinning constituent rather than by the nature of the constituent [2]. Thus in Nb-40% Zr tapes large quantities of second phase dispersed over a range of 2000 to 3000Å [2] produced a structure which supported a J_c in excess of 10 kA/mm^2 at 4.2 K. A similar value for J_c was obtained in Nb-25% Zr wires [3] where the J_c was mainly determined by a well-defined polygonized dislocation structure rather than by a precipitate [4].

The treatments administered to produce both of these desired structures involved annealing highly deformed material under conditions which produced constitutional equilibrium in the materials. Love and Picklesimer [5] have shown that the rate of the equilibrium reaction is very slow in undeformed Nb-25% Zr and Nb-33% Zr, but is increased by a factor of 10 and 15 with 90% deformation. The dislocation structure not only provides elastic energy to aid the diffusion processes, but also acts as nucleation sites for the precipitation reaction. In view of this, it seemed desirable to study how the quantity of deformation introduced into Nb-Zr alloys can influence the maximum J_c which is obtained after subsequently annealing the material. This paper describes this work on two alloys, Nb-26% Zr and Nb-32% Zr. In addition some interesting conclusions can be drawn about the structures needed to produce the highest critical current densities in the Nb-Zr system.

2. Experimental details

2.1. Specimen preparation

The starting materials for this work were slices cut from as-cast, electron-beam melted ingots of Nb-32% Zr and Nb-26% Zr, 40 mm in diameter. The ingots contained the following interstitial impurities; oxygen 220 to 270 ppm; nitrogen 23 to 27 ppm; hydrogen 5 to 8 ppm. A small degree of coring was evident in the starting material.

*Now at Physics Department, Monash University, Clayton 3168, Victoria, Australia.

While it would have been preferable to use homogenized material for this investigation, all attempts to effect this by solution treatment at 1600°C produced material which failed because of intergranular cracking after less than 5% deformation.

The as-cast material was cold rolled, keeping the rolling direction constant, by various amounts up to 96% area reduction, at which stage the material was as thin as could be tolerated for the subsequent work. Pieces, which were cut from the sample at the various stages of deformation, were thinned by lapping to about 200 μm, taking care to maintain the faces parallel. The faces were given a final polish on 1 μm alumina, and a number of magnetization specimens, 3 × 2 mm, were cut from each piece. To categorize the specimens at this stage and ensure there were no compositional fluctuations on a macroscopic scale, the superconducting transition temperature T_c, of each was measured. Although the transitions varied systematically with deformation [6], for each set of specimens of a given amount of deformation they were constant to within ± 0.03 K, the accuracy of the measuring apparatus. This indicated a good level of homogeneity.

A standard annealing time of 1 h was used throughout this investigation. Annealing was done in a dynamic vacuum of less than 5×10^{-6} mm Hg, with each specimen wrapped individually in tantalum foil. The furnace was arranged to roll forward or back over the specimens so that the time taken for them to warm up or cool down was minimized.

The specimens will be described in the following text accordingly: 32/41/650/1 describes a Nb-32% Zr specimen, deformed 41% and annealed at 650°C for 1 h.

2.2. Superconductivity measurements

Measurements of magnetization, M, and remanent flux, B_0, versus field, H, were performed on each specimen at 4.2 K to provide the data necessary for the calculation of the critical state parameters n and α, where

$$\mu_0 j_c = \frac{\alpha}{b^{n-1}}$$

describes the critical state within the material. j_c and b are the local critical current density and induction respectively. μ_0 is the permeability of free space, n and α are material constants. The details of the technique and computation have been described previously [7]. An equivalent critical current density, J_c, for a 254 μm diameter wire of the material in zero applied field was also computed for each specimen, using the measured constants n and α.

Transition temperatures were measured for each specimen using the mutual inductance technique at a frequency of 1200 Hz.

2.3. Metallography

Both optical and electron microscopy were performed on the actual specimens used for the superconducting measurements. The optical microscopy was performed on both etched and anodized surfaces. The details of the anodizing procedure have been reported elsewhere [8] and in many instances this technique provided information on the metallurgical state of the whole specimen which would have been otherwise unobtainable. The wafers were thinned for transmission electron microscopy both by electrolytic and ion-beam thinning. Electrolytic thinning became more difficult as the annealing temperature was increased.

3. Results

3.1. Superconductivity results

A selection of the measured magnetization and remanent flux versus field curves for the Nb-32% Zr alloy before and after annealing at 700°C for 1 h are reproduced in Fig. 1 and the computed critical current densities are plotted in Fig. 2. The results given here were taken with the applied magnetic field parallel to the rolling direction in the rolling plane. However, measurements on a number of specimens have shown that there is no difference between these results and those obtained with the field perpendicular to the rolling direction in the rolling plane.

Figs. 1 and 2 show the following. (1) Magnetic irreversibility and J_c increased systematically with deformation for the material in the unannealed condition. (2) Annealing from the as-cast state increased the magnetic irreversibility, but there was only a slight increase in J_c. (3) For all the deformed specimens a peak J_c was achieved by annealing in the region 700 to 800°C. These peak values are presented in Table I. Beyond 80% deformation the magnitude of this peak J_c remained constant despite the higher initial deformation.

A comparable set of results was obtained for the Nb-26% Zr alloy except that the magnitude of the peak value of J_c was lower than that for the

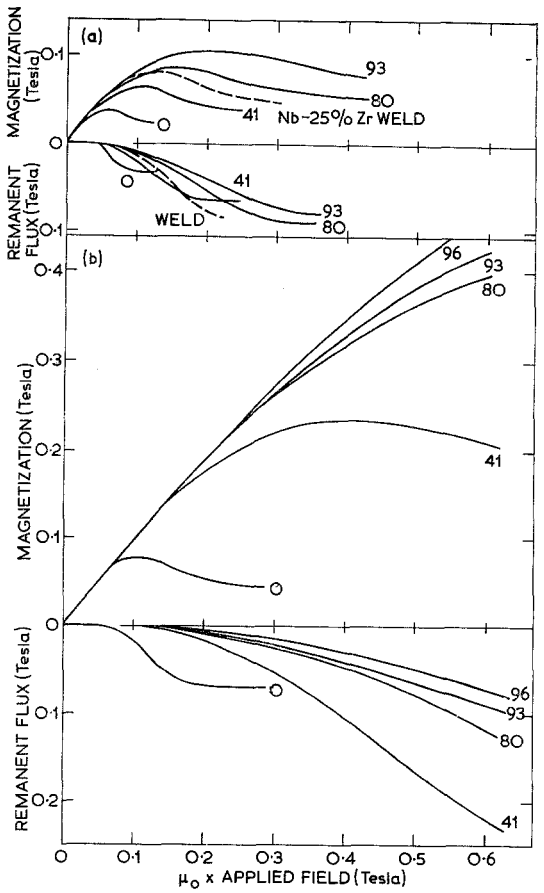

Figure 1 Magnetization and remanent flux versus applied field for Nb-32% Zr specimens (a) before annealing (b) annealed at 700°C for 1 h. The figure by each curve denotes the amount of deformation given to the specimen.

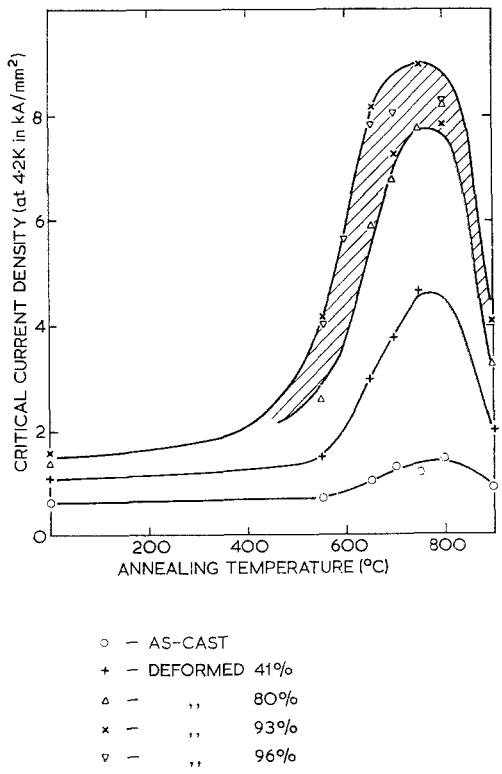

Figure 2 Critical current density computed for an equivalent 254 μm wire, versus annealing temperature for Nb-32% Zr.

Nb-32% Zr alloy. The results for the Nb-26% Zr alloy are also collected in Table I.

The transition temperatures of the Nb-32% Zr specimens are plotted in Fig. 3 from which the variation of T_c with deformation in the unannealed condition can be seen. After an anneal at about 600°C, T_c was independent of initial deformation, but annealing treatments above 600°C caused a separation of the T_c's into two sets, depending on deformation. The as-cast and 41% deformed material followed one T_c versus annealing temperature curve and the highly deformed material another, somewhat higher. The transition widths, as defined in the inset to Fig. 3, were constant for each set of annealed specimens and have been indicated on the figure.

Deformation of the as-cast Nb-26% Zr alloy also caused a systematic increase in T_c, from 10.41 to 10.92 K after 93% deformation. After annealing above 700°C, the T_c's for all deformations coincided to within a transition width and above 750°C the transition temperatures for these specimens also coincided with those of the highly deformed Nb-32% Zr alloy.

TABLE I

Specimen	T_c (K)	J_c (kA/mm²)
32/as-cast/800/1	10.47	1.5
32/41/750/1	10.41	4.6
32/80/800/1	10.65	8.2
32/93/750/1	10.68	8.9
32/96/800/1	10.56	8.3
26/as-cast/800/1	10.78	1.3
26/45/750/1	10.65	3.0
26/82/800/1	10.69	5.1
26/93/800/1	10.70	5.6

3.2. Metallurgical structure

Structurally there was little difference between

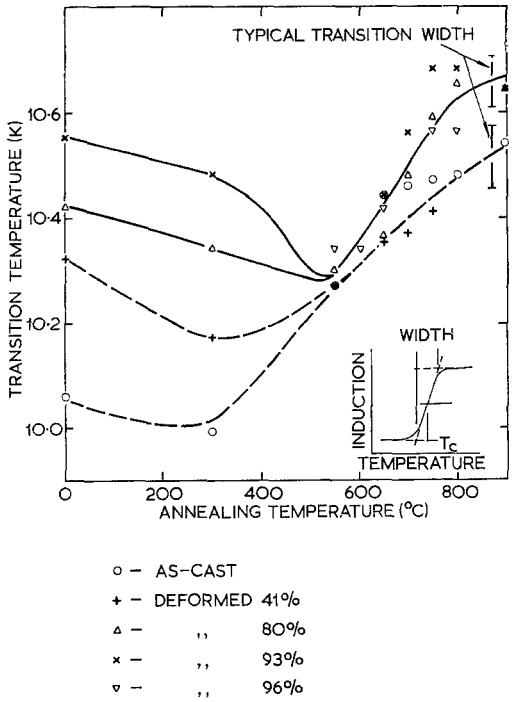

Figure 3 Transition temperature of Nb-32% Zr versus annealing temperature.

specimens containing 32% Zr and those containing 26% Zr after equivalent treatments, except that the quantity of precipitation, once it had occurred, was larger in the former alloy. For this reason optical micrographs of the Nb-26% Zr were not as complex as those of the Nb-32% Zr.

The small degree of coring, evident in the as-cast specimens, was accompanied by occasional precipitates of β_{Zr}, mainly in the grain boundaries, but also scattered across the grains and between the dendrites. Annealing this structure did not modify it. Rolling progressively broke up the grains and the coring so that after 80% reduction in area, little could be seen of the original structure.

Precipitation of β_{Zr} occurred on annealing the rolled specimens at any temperature above 600°C. While this precipitate was most easily identified by anodizing, it was also revealed by etching. It always appeared to have nucleated heterogeneously, decorating the slip bands of specimens deformed about 40% and the areas of high dislocation density of specimens containing more cold work. This can be clearly observed in Fig. 4 where the deformation in a specimen reduced 45% was confined to simple slip patterns (Fig. 4a) while that in a specimen reduced 93% was more

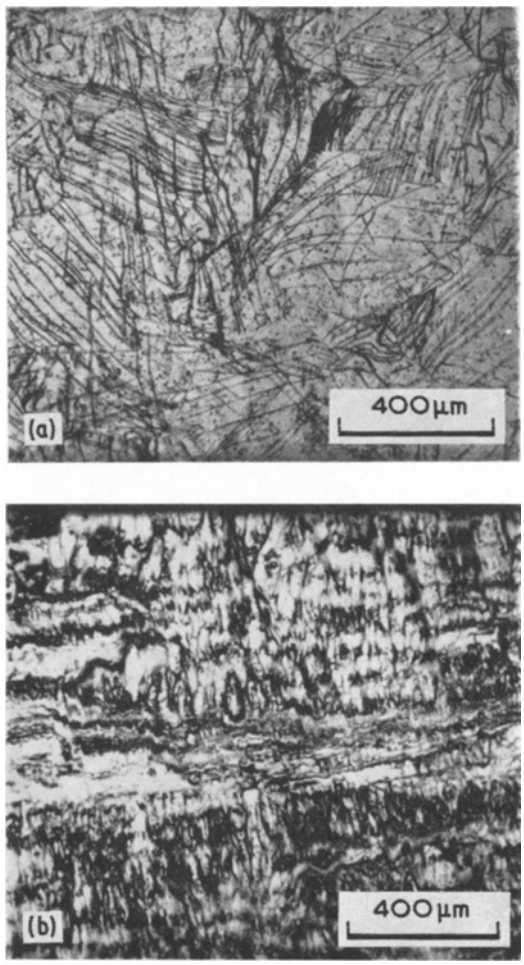

Figure 4 Optical micrographs of Nb-26% Zr deformed (a) 45% and (b) 93% then annealed at 750°C for 1 h.

generally distributed (Fig. 4b). Specimens deformed 80% had a similar but slightly coarser structure than those deformed above 90%.

Annealing temperatures above 650°C did not noticeably influence the quantity of β_{Zr} precipitated, as can be seen by comparing Fig. 5a with Fig. 4b. The structure always appeared to contain regions comparatively free from precipitate bounded by walls containing a mixture of β_{Zr} precipitate and β_{Nb}. Similar precipitate-free regions were observed in the edge view of the specimen, Fig. 5b, although the structure was on a much finer scale (note the difference in magnification between Figs. 5a and b). The precipitate-free regions were no more than 4 μm thick.

The low magnifications illustrated in Figs. 4 and 5a gave a clear indication of the distribution

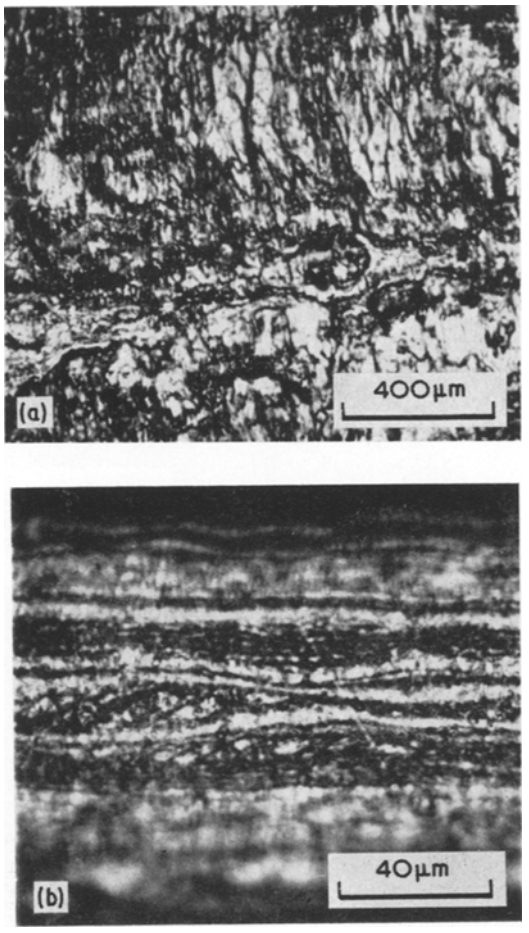

Figure 5 Optical micrographs of Nb-26% Zr deformed 93% then annealed at 700°C for 1 h. (a) Structure parallel to rolling plane. (b) Structure perpendicular to rolling plane and rolling direction.

of the precipitate. Higher magnifications, especially of structure parallel to the rolling plane, tended to produce diffuse images which were more difficult to understand. For example the difference in precipitate quantity between the 32/93/700/1 specimen and the 26/93/700/1 specimen can be most clearly seen by comparing the low magnification micrographs of Figs. 5a and 6. The sample containing the larger quantity of Zr exhibited the greater amount of precipitate.

Examination of these specimens by transmission electron microscopy confirmed the observations made optically. No precipitation was ever observed in the unannealed deformed specimens, only a uniform density of dislocations which showed little tendency to tangle or form cells. Once the specimens had been annealed,

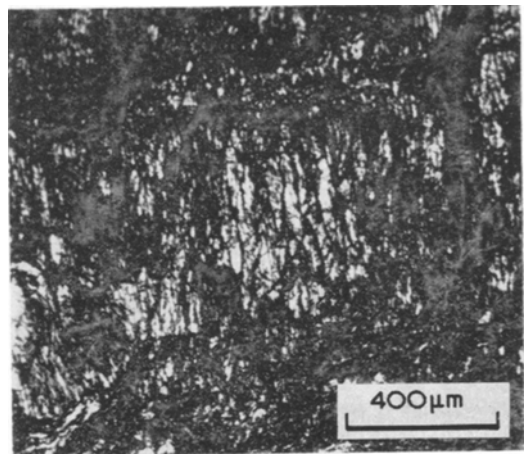

Figure 6 Optical micrograph of Nb-32% Zr deformed 93% then annealed at 700°C for 1 h.

however, β_{Zr} was readily observed in the diffraction patterns, although it was only in specimens containing the higher quantities of deformation that it could be considered to be a general feature of the microstructure. In this condition specimens deformed in the region of 40% exhibited several areas of uniform dislocation density like that shown in Fig. 7. Any precipitate present was lost within this structure and could not even be observed in the diffraction patterns. Other areas of the specimen which might have contained precipitate on a scale

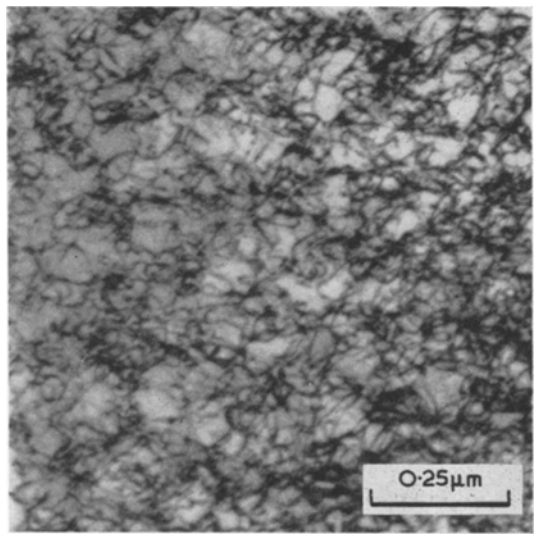

Figure 7 Electron transmission micrograph of Nb-32% Zr deformed 41% then annealed at 700°C for 1 h.

visible in the electron microscope had not been satisfactorily thinned – a consequence of the lack of uniformity of the structure. Even in specimens deformed as much as 93% it was possible to observe some areas which did not contain precipitate.

The non-uniformity of the structures of these specimens is further exemplified in Fig. 8 where an area of 32/92/650/1 is shown containing a high dislocation density, and an area of the same specimen in which new grains can be observed to

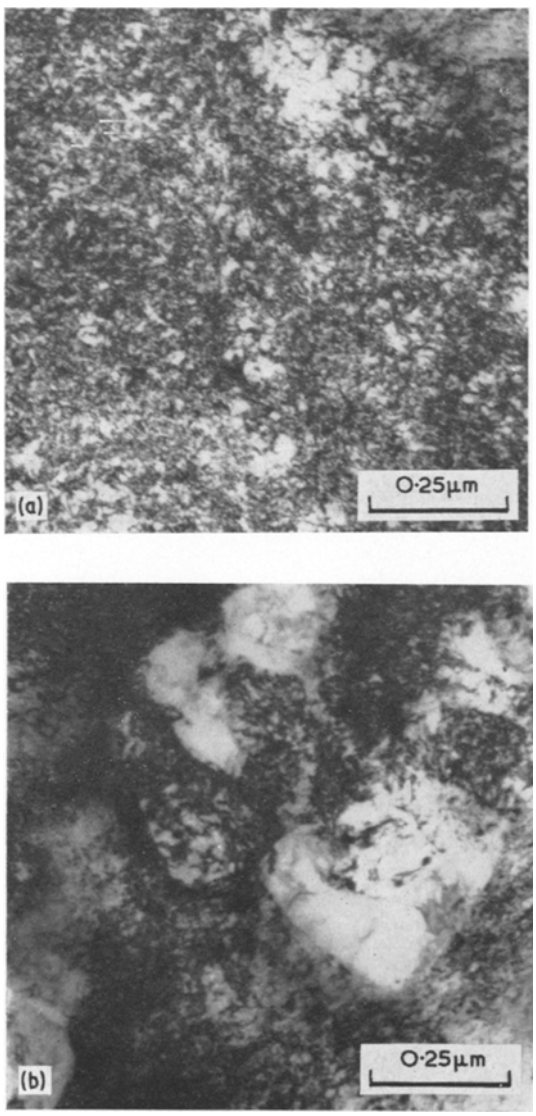

Figure 8 Electron transmission micrographs of Nb-32% Zr deformed 93% then annealed at 650°C for 1 h.

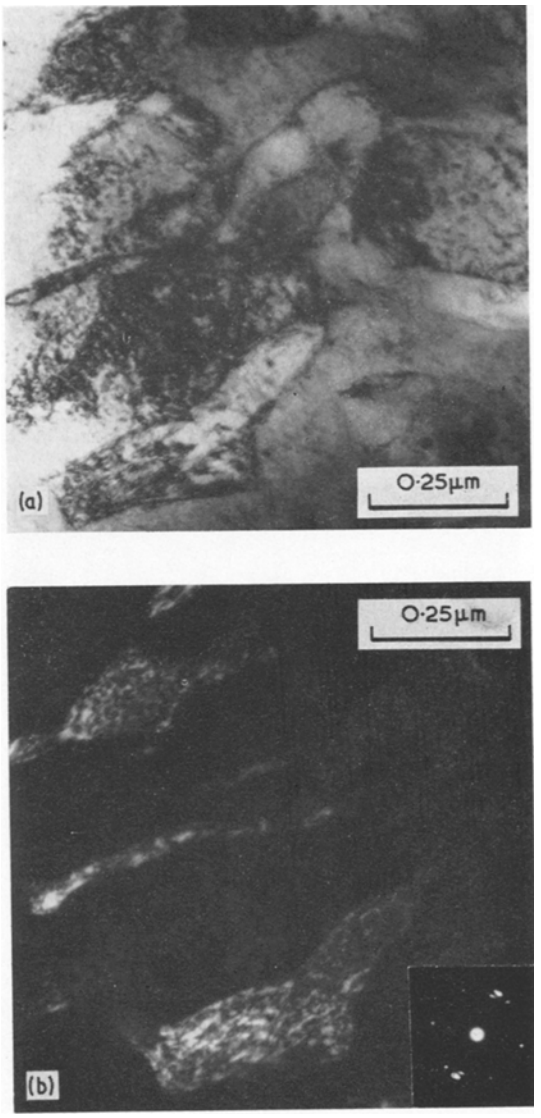

Figure 9 Electron micrographs of Nb-32% Zr deformed 93% then annealed at 700°C for 1 h. (a) Bright field image. (b) Dark field image using β_{Zr} reflection.

be growing. Specimens annealed at higher temperatures exhibited similar variations in structure, but with a larger and more variable grain size. Dark field electron microscopy using a β_{Zr} reflection (Fig. 9) showed that the β_{Zr} in the recrystallized regions was contained in a structure developing in the grain boundaries rather than precipitating as discrete particles within the grains.

4. Discussion

4.1. Microstructure

The outstanding feature about the material of this study is the lack of uniformity in the structure. Although the transition temperature widths indicated a reasonable degree of compositional homogeneity in the samples, which was substantiated by the anodic metallography on the unannealed specimens, precipitate was unevenly dispersed in all of the annealed specimens.

Because of the sensitivity of the precipitation kinetics to plastic deformation in this system, regions of a specimen containing a high density of deformation debris, such as the slip planes of a sample deformed 45%, would be expected to cause a local rapid rate of precipitation. Consequently, in short term anneals (e.g. 1 h), lightly deformed material would not be expected to fully decompose so that precipitation would occur only on the slip planes producing the structure observed in Fig. 4a. When deformation is spread more evenly throughout the sample, as in specimens deformed 80 and 90% the precipitate would again be distributed in a manner determined by the pattern of deformation. This makes the precipitate a useful indicator of the uniformity of deformation in these samples.

The structures observed parallel to the rolling plane (Figs. 4, 5a and 6) were very much coarser than those viewed perpendicular to this (Fig. 5b), a consequence of the anisotropy of the rolled structure. Because of the orientation in which the specimens were measured it is the scale of these features perpendicular to the rolling plane which determines the flux pinning characteristics.

The work which has been published to date on deformed structures of bcc metals indicates that a cell structure similar to that observed in fcc materials often develops after deforming as little as 2% [9-11]. This cell structure is sensitive to the temperature of deformation, to the amount of deformation and to the alloying constituent, probably because of the way these factors can influence the width of the dislocations and their ability to cross-slip and climb.

The dislocation structures observed in any of the specimens thinned for electron microscopy showed no tendency to form cells, or to arrange themselves in a polygonized structure. The simple structures observed optically after about 40% deformation suggest that cross-slip is extremely difficult in this material, a factor which would inhibit cell formation, and also account for the reluctance of this material to deform plastically. Larger quantities of deformation would naturally force the dislocations to cross-slip and distribute the deformation more evenly throughout the specimen.

Annealed specimens contained not only precipitate, but also new grains. Specimens which produced the highest J_c consisted mainly of regions containing both, with the β_{Zr} precipitated in the grain boundaries in a distribution determined by the size of the new crystals, about 2000 to 3000Å. This is a pattern of precipitation which was observed previously in Nb-40% Zr [2]. The highest annealing temperatures produced structures containing recrystallized grains large enough to be observed optically, and these had low critical current densities.

4.2. Transition temperatures

The variation in the transition temperatures with annealing temperature for both these alloys is complicated by the increase in T_c with deformation. Transition temperatures for Nb-Zr normally reach a peak value of about 11 K near 25% Zr and decrease to 10.7 K at 32% Zr [12]. In the unannealed condition, for both the Nb-26% Zr and the Nb-32% Zr, T_c approached these respective values as deformation was introduced. This suggests that the enhancement of T_c in Nb-Zr by deformation published by Finlayson and Milne [6] may actually be due to a depression of T_c in the as-cast state. However, until the mechanism responsible for this variation of T_c with deformation is firmly established, the reasons for the behaviour of T_c on annealing at low temperatures will remain in doubt.

Previous work on Nb-25% Zr has shown that the minimum in a T_c versus annealing temperature isochronal coincides with the annealing temperature above which equilibrium is achieved in this system [4]. The behaviour of the highly deformed Nb-32% Zr alloy is consistent with this explanation, if it is allowed that the deformation free regions will not begin to decompose unless annealing times much longer than 1 h are employed [5]. Since these regions involve only a small volume of the total they will have an unobservable effect on T_c. No equivalent minimum was observed in the isochronals for the Nb-26% Zr alloy, largely because insufficient data was collected in the relevant region, but the values for T_c in the expected equilibrium region (above 650°C) agree well with the relevant T_c measurements for the Nb-32% Zr.

Values of T_c lower than the equilibrium ones have been obtained for the Nb-32% Zr alloy as-cast and deformed 41% after the 1 h heat-treatments. This implies that equilibrium has not been achieved, a fact which is confirmed by the smaller amounts of precipitation in them than in the highly deformed ones.

4.3. Critical currents in unannealed material

In the as-cast material the critical current density was appreciable, although low by comparison with the peak values achieved. The observable metallurgical features which are normally thought to be responsible for flux pinning, namely precipitates, grain boundaries and compositional fluctuations due to coring, were on a scale too large to be effective, about two orders of magnitude larger than the flux line spacing (about 2500Å at the maximum value of the remanent flux.) The magnetization curve for another as-cast sample, a Nb-25% Zr weld, has been included in Fig. 1a for comparison. An even greater amount of magnetic irreversibility was displayed by this sample. The weld contained a much finer and more evenly distributed cored structure, with larger composition fluctuations, than the specimens studied here. It appears therefore, that despite the scale of the inhomogeneities, coring may be contributing to the pinning of flux and the large critical current densities in the as-cast material.

The continuous increase in magnetic irreversibility and J_c with deformation of the cast structure is consistent with much of the early work on this alloy [13]. However, some later studies on deformed Nb and some Nb alloys [14] showed that this behaviour occurred only until a dislocation cell structure became established. Once the cell size became constant with increasing amounts of deformation, after about 10 to 20% area reduction, the magnetic irreversibility stopped increasing. It seems that the continuous increase in J_c with deformation of the Nb-Zr alloys studied here is related to their inability to form cells when being deformed.

4.4. Critical currents in annealed material

In all of the specimens which had been deformed before annealing, and where enhancement of J_c had occurred after annealing, β_{Zr} precipitate appeared to be the main feature responsible for this. Where the precipitate was evenly distributed throughout most of the specimen there was no difficulty in calculating J_c from the magnetization results. For some of the annealed specimens, however, particularly the as-cast and those containing about 40% deformation, an uneven structure led to the following complications in the analysis of the magnetization data.

1. M/H is expected to be a linear function of B_0/H up to a field in the region of the maximum in the magnetization [7]. Occasionally this was not the case.

2. n is usually between 1 and 2 and α about 10^3 [7]. Occasionally values of n greater than 2 and values of α less than 10^2 were obtained. These parameters are not real physical constants, however and a complementary behaviour is to be expected between them. The quantity of real physical significance, J_c, behaves in a more reasonable way. For example, in the as-cast material J_c changed very little with annealing, while n increased and α decreased. Further experiments are being performed to study the significance of these changes in n and α.

For specimens containing 80% and more deformation the values of J_c obtained after annealing were scattered about a mean curve. The high degree of scatter of experimental points in the peak was caused partly by the inhomogeneities discussed above and partly by uncertainties in the computed material constants. These are always greatest in the region of peak J_c where flux jumps often limit the range of usable magnetization results.

Evidence from the transition temperatures indicates that, at least in the material deformed beyond 80%, equilibrium quantities of β_{Zr} have been precipitated after annealing above about 600°C. The effectiveness of a second phase in pinning flux is not only dependent upon the quantity of precipitate present, however, but also upon its dispersion in the matrix. For example Waldron [15] has shown in Nb-25% Zr that for a given applied field very fine dispersions of β_{Zr} can be more influential in pinning flux than coarser ones. The critical dispersion is related to the flux spacing and hence the value of the applied field, so that a given dispersion of pinning centres can operate efficiently at only one value of the field. In Nb-40% Zr Finlayson and Milne [2] showed that β_{Zr} precipitated by annealing the material for 1 h at 600 to 650°C was on too fine a scale for maximum pinning of flux in low fields. Indeed the most efficient structure for the pinning of flux occurred when the β_{Zr} precipitated in the boundaries of recrystallized grains which were approximately 2000 to 3000Å in diameter.

Similar structures were observed in the specimens studied here which had the highest J_c and it is likely that a similar sequence of precipitation is responsible for the shape of the J_c curves of Fig. 2.

The return of J_c to low values after annealing all the specimens at 850 or 900°C is of some additional interest. In material deformed above 80% it was caused by an increase in the grain size leading to a non-ideal dispersion of β_{Zr} precipitate. However, in material deformed only 40%, an increase in the annealing temperature of these specimens above about 750°C was expected to induce more of the supersaturated solid solution to decompose and lead to a higher J_c. That it did not is a good testimony to the observations of Love and Picklesimer [5] regarding the sensitivity of the kinetics of this decomposition to the amount of deformation available in the lattice. However, where this deformation was available, on slip planes, annealing at the higher temperatures led not only to precipitation, but also to a larger local grain size than that required to maximize J_c. This resulted in a decrease in J_c with annealing at temperatures above 750°C.

TABLE II

Alloy	Maximum J_c after 1 h anneal (kA/mm²)	Annealing temperature (°C)
Nb-25% Zr [3]	13.2	750
Nb-26% Zr	5.6	800
Nb-32% Zr	8.9	750
Nb-40% Zr [2]	12.1	800

The magnitude of the maximum J_c attained in each alloy is compared in Table II with that for Nb-25% Zr drawn 99.85% [3] and that for Nb-40% Zr deformed 90% [2]. The lowest J_c occurred in the Nb-26% Zr material, a value which was only half of that obtained in either the Nb-25% Zr or the Nb-40% Zr. The microstructure of the Nb-40% Zr contained approximately 50% precipitated phase when it was in the high J_c condition. The Nb-32% Zr and Nb-26% Zr studied here, on the other hand, contained much less precipitate than this.

With smaller amounts of precipitate it is not surprising that the structures do not support such a high critical current density. Where large volume fractions of precipitate are not available, a high J_c can be obtained only if dislocations in the deformed material can be made to polygonize and produce the structure observed by Milne [4] in the Nb-25% Zr wires. In the present experiments, precipitation was of such a quantity that, occurring heterogeneously, it prevented the dislocations from polygonizing into the necessary structure.*

5. Conclusions

1. Nb-26% Zr and Nb-32% Zr in the as-cast state supported a critical current density which appeared to be controlled by the scale of the coring in the structure, but was not increased appreciably by annealing the material.
2. Deforming the as-cast structures caused a significant increase in magnetic irreversibility and J_c.
3. Critical current densities in deformed material were increased to a peak value by annealing near 750°C for 1 h, regardless of the amount of deformation. The highest J_c was obtained for specimens deformed more than 80%, but further deformation did not cause any extra increase.
4. The flux pinning agent mainly responsible for the highest critical current densities was β_{Zr} precipitated in the boundaries of grains 2000 to 3000Å in size.
5. The maximum J_c obtained in Nb-26% Zr was lower than in Nb-32% Zr because there was less precipitate available for flux pinning.
6. Precipitation was heterogeneous and occurred on slip planes as well as in grain boundaries. Thus in lightly deformed material equilibrium was not attained and the peak J_c's were low.

Acknowledgements

This work was carried out at the Central Electricity Research Laboratories and the paper is published by permission of the Central Electricity Generating Board. We are grateful to the Fabrication Section of the Scientific Services Department, South Eastern Region Laboratories of the CEGB for supplying the rolled alloys.

References

1. M. T. TAYLOR, Commission 1, London, Annex 1969-1, *Bull I.I.R.* (1969) 119.
2. T. R. FINLAYSON and I. MILNE, *Phil. Mag.* **25** (1972) 1291.
3. I. MILNE and D. A. WARD, *Cryogenics* **12** (1972) 176.

*The very small volume fraction of precipitate observed in the Nb-25% Zr by Milne is thought to be a result of the unusually low oxygen content of this material.

4. I. MILNE, *J. Mater. Sci.* **7** (1972) 413.
5. G. R. LOVE and M. L. PICKLESIMER, *Trans. AIME* **236** (1966) 430.
6. T. R. FINLAYSON and I. MILNE, *Sol. State Com.* **9** (1971) 1339.
7. J. SUTTON and D. A. WARD, *J. Phys. D.* **5** (1972) 628.
8. T. R. FINLAYSON and I. MILNE, Inst. of Mets. Conf. on Modern Metallog. in Metall., Liverpool, September, 1971.
9. A. S. KEH and S. WEISSMANN, "Electron Microscopy and Strength of Crystals", Ed. G. Thomas and J. Washburn (Interscience, New York, 1963) 231.
10. R. BENSON, G. THOMAS, and J. WASHBURN, "Direct Observation of Imperfections in Crystals", Ed. J. B. Newkirk and J. H. Wernick (Interscience, New York, 1961) 375.
11. M. J. WITCOMB, A. ECHARRI, A. V. NARLIKAR, and D. DEW-HUGHES, *J. Mater. Sci.* **3** (1968) 191.
12. J. K. HULM and R. D. BLAUGHER, *Phys. Rev.* **123** (1961) 1569.
13. K. M. OLSEN, R. F. JACK, E. O. FUCHS, and F. S. L. HSU, "Superconductors", Ed. M. Tanenbaum and W. V. Wright (Interscience, New York, 1962) p. 126.
14. A. V. NARLIKAR and D. DEW-HUGHES, *J. Mater. Sci.* **1** (1966) 317.
15. G. W. J. WALDRON, *ibid* **4** (1969) 290.

Received 27 March and accepted 17 May 1972.